International Journal of Geo-Information

MDPI

Article

Identification of Urban Agglomeration Spatial Range Based on Social and Remote-Sensing Data—For Evaluating Development Level of Urban Agglomeration

Shuai Zhang [1] and Hua Wei [2,*]

[1] School of Architecture and Urban Planning, Yunnan University, Kunming 650500, China
[2] School of Innovation and Entrepreneurship, Zhengzhou College of Finance and Economics, Zhengzhou 450044, China
* Correspondence: weihua@zzife.edu.cn

Abstract: The accurate identification of urban agglomeration spatial area is helpful in understanding the internal spatial relationship under urban expansion and in evaluating the development level of urban agglomeration. Previous studies on the identification of spatial areas often ignore the functional distribution and development of urban agglomerations by only using nighttime light data (NTL). In this study, a new method is firstly proposed to identify the accurate spatial area of urban agglomerations by fusing night light data (NTL) and point of interest data (POI); then an object-oriented method is used by this study to identify the spatial area, finally the identification results obtained by different data are verified. The results show that the accuracy identified by NTL data is 82.90% with the Kappa coefficient of 0.6563, the accuracy identified by POI data is 81.90% with the Kappa coefficient of 0.6441, and the accuracy after data fusion is 90.70%, with the Kappa coefficient of 0.8123. The fusion of these two kinds of data has higher accuracy in identifying the spatial area of urban agglomeration, which can play a more important role in evaluating the development level of urban agglomeration; this study proposes a feasible method and path for urban agglomeration spatial area identification, which is not only helpful to optimize the spatial structure of urban agglomeration, but also to formulate the spatial development policy of urban agglomeration.

Keywords: Central Plains Urban Agglomeration (CPUA); nighttime light; urban expansion; spatial range; big data

Citation: Zhang, S.; Wei, H. Identification of Urban Agglomeration Spatial Range Based on Social and Remote-Sensing Data—For Evaluating Development Level of Urban Agglomeration. *ISPRS Int. J. Geo-Inf.* **2022**, *11*, 456. https://doi.org/10.3390/ijgi11080456

Academic Editors: Hangbin Wu and Tessio Novack

Received: 2 July 2022
Accepted: 18 August 2022
Published: 21 August 2022

1. Introduction

In the study of human settlements, an urban agglomeration is an extended city or town area comprising the built-up area of a central place and any suburbs linked by a continuous urban area [1,2]. Urban agglomeration occurs when the relationships among cities shift from mainly competition to both competition and cooperation [3,4]. Cities within an urban agglomeration are highly integrated, rendering the agglomeration one of the most important carriers for economic development. The formation of an urban agglomeration often signifies a highly developed economic and modernization level in a region, which can bring enormous benefits because of the scales of economics [5,6].

Recently years, as the world's second-largest economy, the Chinese government has proposed many strategies to actively promoting and developing urban agglomeration [7], which clearly indicating that the urban agglomeration is likely to be the viable future spatial organization of urban and the driving force of urban development in China [8]. What is well-known is that urban agglomeration is a huge, complex and dynamic system, which is typically characterized by time-efficient (the development level of the same urban agglomeration could be significantly different in different periods) and regional (in one period, different urban agglomeration would undoubtedly be branded with the local mark). Therefore, one of the most important contents in studying urban agglomeration is to judge

its development level [9]. The mainly way of judging the development level of urban agglomeration still lies on relying on the adaptation of statistic data and administrative regions [10], which can no longer meet the need of accurately and fundamentally judge the development level at present [11]. Additionally, the influence range in the actual development process of different urban agglomeration is of great differences, which made it possible for scholars to judge urban agglomeration development level by identifying its influence range, so as to achieve effective management and thus achieve sustainable development of urban agglomeration [12].

As one of the most important spatial data that reflecting urban geographical information, remote-sensing data is characterized by higher resolution, wider coverage, quicker pick-up speed, as well as rapider update, compared with traditional statistic survey data, which all rendering it as one of the most important data on judging urban spatial development level [13–15]. NTL (nighttime light data), one type of remote-sensing data, is the data that could most directly evaluate the urbanization level due to its only attribution of reflecting the spatial distribution trend of urban infrastructure as well as reflecting the level of human activity by capturing nighttime data during the urban night [16]. Although NTL data, including DMSP/OLS (Defence Meteorological Program Operational Line-Scan System), NPP/VIIRS (Suomi National Polar-orbiting Partnership/Visible Infrared Imaging Radiometer Suite), as well as has Luojia-01 all has been intensively studied and widely used in identifying urban area, delineating urban agglomeration boundary, extracting urban built-up area as well as in comparing the development level of different urban cities [17–19], it is still needed to figure out the emphasis of different type of NTL data. Firstly, DMSP/OLS NTL data offering data with 1000 m spatial resolution from 1992 to 2013. Due to the limitation of the time scale, DMSP/OLS NTL data are less used in the current urban space studies [20]. Secondly, NPP/VIIRS NTL data has a higher spatial resolution of 500 m compared with DMSP/OLS NTL data. Besides, NPP/VIIRS NTL data could timelessly offer NTL data since 2013, which contributes to the fact that the applied study of NTL data at present mainly focus on NPP/VIIRS NTL data [21]. Thirdly, Luojia-01NTL data, provided by Wuhan University of China from October 2018 with a spatial resolution of 130 m. Although the higher spatial resolution of Luojia-01NTL data made it superior in relevant urban space study, the fact that it stopped updating NTL data since the beginning of 2020 made it more widely used in the study from 2018 to 2020 [22].

In the study of using NTL data to identify the urban area and extract urban built-up area, it is of great importance to set different light threshold value since different threshold would make a significant difference on the study results [23,24]. In the previous studies, the relatively accurate method of selecting threshold value is dichotomy [25], that is, constantly dichotomia the nighttime light data until the obtained threshold most close to the true value; however, the fact that dichotomy only could be used by a researcher who is familiar with the study area makes it failed to qualify to be popularized [26]. Recent years, the development of new methods such as machine learning and object-oriented method enables image to be more effectively segmented. Although it has been proved in many studies that with the object-oriented image-segmentation method, more accurate results could be obtained. The urban area that NTL data could identify is still the area that covered by nighttime lights, which means that the single-source NTL data could no longer accurately reflect the influence range of urban space [27,28].

In recent years, with the emerging of urban big data study, big data based on location service has been playing an increasingly important role in urban-related studies, which contributes to the existence of a unique perspective for an investigation into the observation of human-centered spatial activity within urban space [29–31]. As one of the emerging geographical spatial big data, POI (point of interest) data offers an abstract representation of geographical entities in virtual space with the advantage of wider coverage and faster updating speed [32]. POI data are expressed as a point vector data set within the geographical information system, which can be used to express the internal spatial structure within urban space. At present, although POI data has been widely used in studies of the extrac-

tion of urban build-up areas, the identification of urban centers, the spatial distribution of population, as well as the delineation of urban boundaries [33,34], its only attribute (POI data only offers the name as well as latitude and longitude of object) has also resulted in the fact that the application of POI data pays more attention to some certain spatial functions such as "the used" space within urban area [34].

NTL data reflects the coverage area of urban light, while POI data mainly reflects the used urban space within urban area, so there is a significant correlation between NTL data and POI data in urban space [35]; it has also been reflected by previous studies that fusing these two kinds of data can significantly improve the accuracy of studies on urban-related studies in terms of identifying urban center, delineating urban-rural boundary and identifying urban-rural area [36–40]. Current studies mainly focus on large urban agglomerations such as the Yangtze River Delta and the Pearl River Delta [41,42], while less attention is paid to cities with a general level of urban development, additionally, most studies on the fusion of NTL data and POI data mostly take POI data as a supplement to NTL data; however, the difference between POI data and NTL data lies in that NTL data reflects regional differences in urban development [43,44], while POI data reflects the spatial distribution of urban space.

Single datum cannot fully reflect the formal situation of urban space in the process of application, which makes the application of data fusion become one of the important contents of urban-related studies. Data fusion refers to the combination and transformation of the information obtained from different channels of single-source or multi-source data. After data fusion, the fused information could provide more accurate and complete estimation and judgment than the single-source data, so as to reduce the prediction error and improve the reliability of data application [45,46].

In this study, to accurately estimate the development level of Central Plains Urban Agglomeration (CPUA), the data fusion method was firstly used to fuse NTL data and POI data; then in order to more accurately determine the influence range of CPUA so as to provide a more reliable abstraction methods and flow path of spatial influence range of urban agglomeration, the identification results obtained by the fused NTL&POI data is comparatively analyzed and verified with that obtained by single-source NTL data and that of single-source POI data. Compared with other relevant studies, the contribution of this study mainly lies in choosing CPUA as the, which has an average level of urban development but a relatively fast development speed. Choosing the study area in the CPUA with a general urban development level but a rapid development speed. On the one hand, it can verify whether the study method can achieve the expected effect in areas with less urban built-up areas, thus enriching the theoretical studies on urban area. On the other hand, the accurate identification results obtained in this study are helpful to judge its development level, so as to provide a scientific basis for promoting the balanced coordination and development of regional space within the urban agglomeration. Finally, this study uses two indicators to compare the accuracy of different data in identifying urban and rural spatial ranges. The first one is accuracy, which represents the percentage of the total number of points successfully verified in urban and non-urban areas for different data in the identification of urban and rural spaces. The second is the Kappa coefficient, which represents the classification accuracy of urban and rural spaces, ranging from -1 to 1, the closer the value is to 1, the higher the classification accuracy would be.

2. Materials and Methods

2.1. Study Area

Located in central and eastern China with Henan Province as the main body, CPUA is an urban agglomeration with the densest population, strong economic strength, rapid industrialization process, high level of urbanization, and prominent transportation location advantages in central and eastern China (Figure 1). With a total area of 287,000 square kilometers, including 30 prefecture-level cities, the results of the seventh census show that the population of CPUA reached 160 million, all making it one of the most important urban

economic growth poles in central China [47]. Additionally, compared with the results of the sixth census, the population of CPUA has increased by more than 30%, and by the results of the seventh census, the population of CPUA has exceeded that of the major coastal urban agglomeration in China. Therefore, accurate identification of the spatial influence range of CPUA is helpful to judge its development level, so as to formulate reasonable urban agglomeration development policies and provide a reasonable reference for the healthy development of other urban agglomerations of the same type.

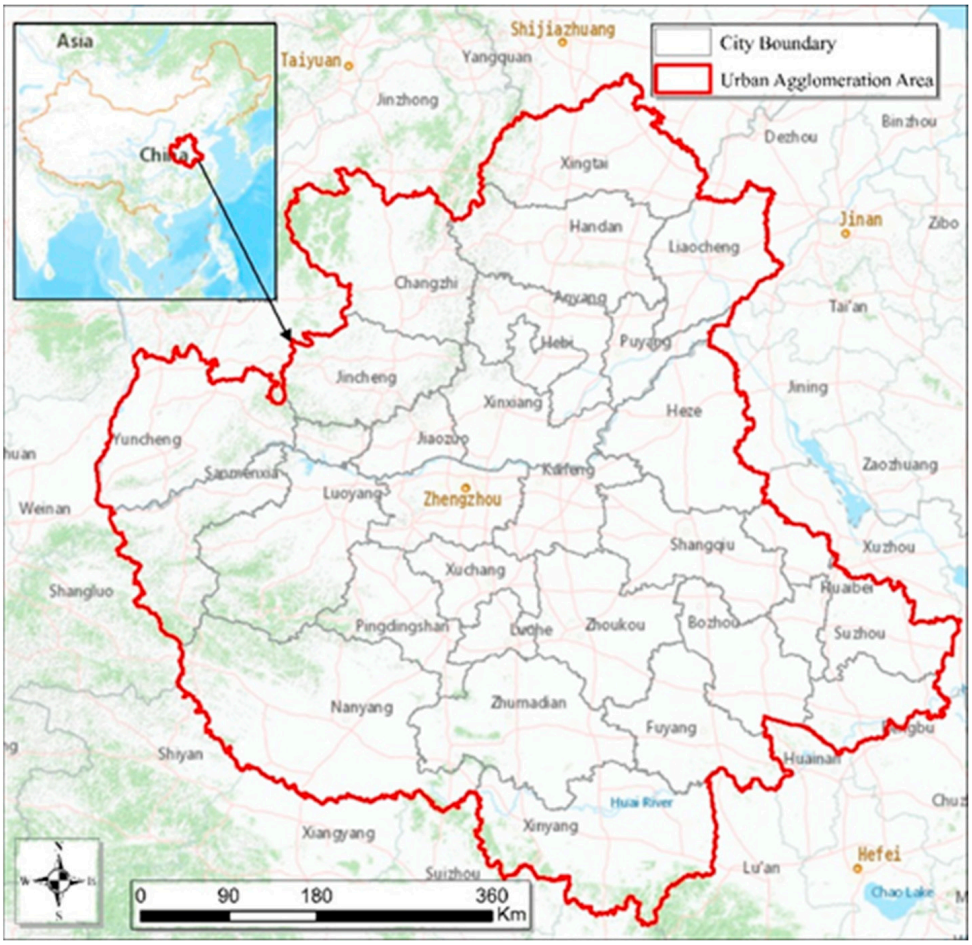

Figure 1. Central Plains Urban Agglomeration.

2.2. Study Data

The data used in this study mainly include NPP/VIIRS NTL data and POI data. The specific acquisition methods and processing processes of different data are as follows.

NPP/VIIRS NTL data, with a spatial resolution of 500 m and a width of 3000 km, is provided by the Suomi NPP and NOAA-20 satellites that were launched by NASA. Compared with DMSP/OLS NTL data, NPP/VIIRS data has a more significant advantage in spatial scale analysis, allowing for a more detailed representation of numerical characteristics. Additionally, the more complete global coverage and higher time quality data all make it possible for NPP/VIIRS data to provide more detailed examination in the study of urban interior spatial structure, which in turn greatly improves the accuracy of urban space identification [48,49]. At present, NPP/VIIRS data can be downloaded from https://eogdata.mines.edu/products/vnl/ (accessed on 30 April 2022) for free. NPP/VIIRS NTL data of CPUA from January to December 2021 can be obtained by visiting the website and the pre-processing results of NTL data in CPUA (Figure 2) can be obtained after radiative correcting and monthly average processing of the obtained data,

the monthly average processing is carried out to avoid the possible differences caused by light anomalies in a single month.

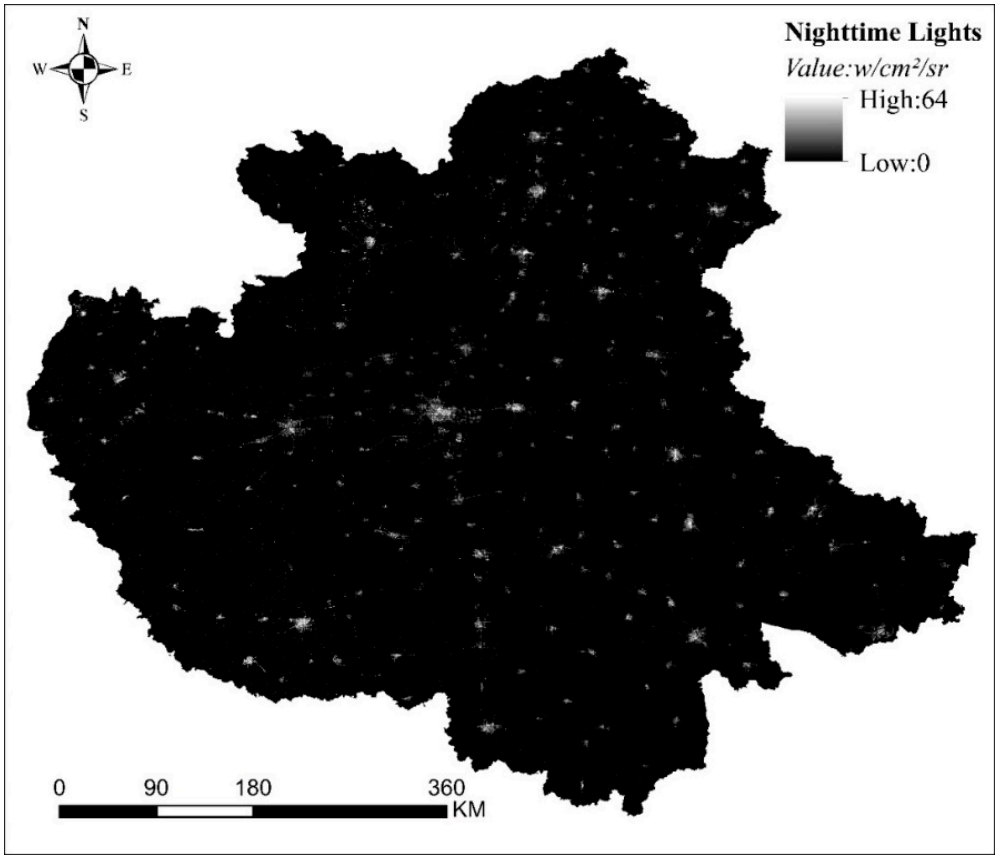

Figure 2. Pre-processing Results of NTL data in CPUA.

As a data set of spatial location-specific point, POI (Point of Interests) data has four basic attributes: name, address, coordinates, category, which are integrated and expressed as point vector data set in the geographic information system (GIS). The aggregation distribution of POI data can be used to calculate the distribution of infrastructure in urban space and urban internal spatial structure, which makes POI data widely used in urban-related studies [50]. At present, map service providers, including Baidu Map, Amap and Google Map, have developed and provided Application Programming Interface (API) access services, which allow users to access various types of open data. By visiting Amap API (www.amap.com) (accessed on 1 January 2022), the number of POI data in CPUA by December 2021 obtained by this study is 129,822,14. After re-checking, cleaning and screening the obtained POI data, the total number of POI data in CPUA is 812,639,1. The quantity and spatial distribution of POI data in CPUA are shown in Figure 3.

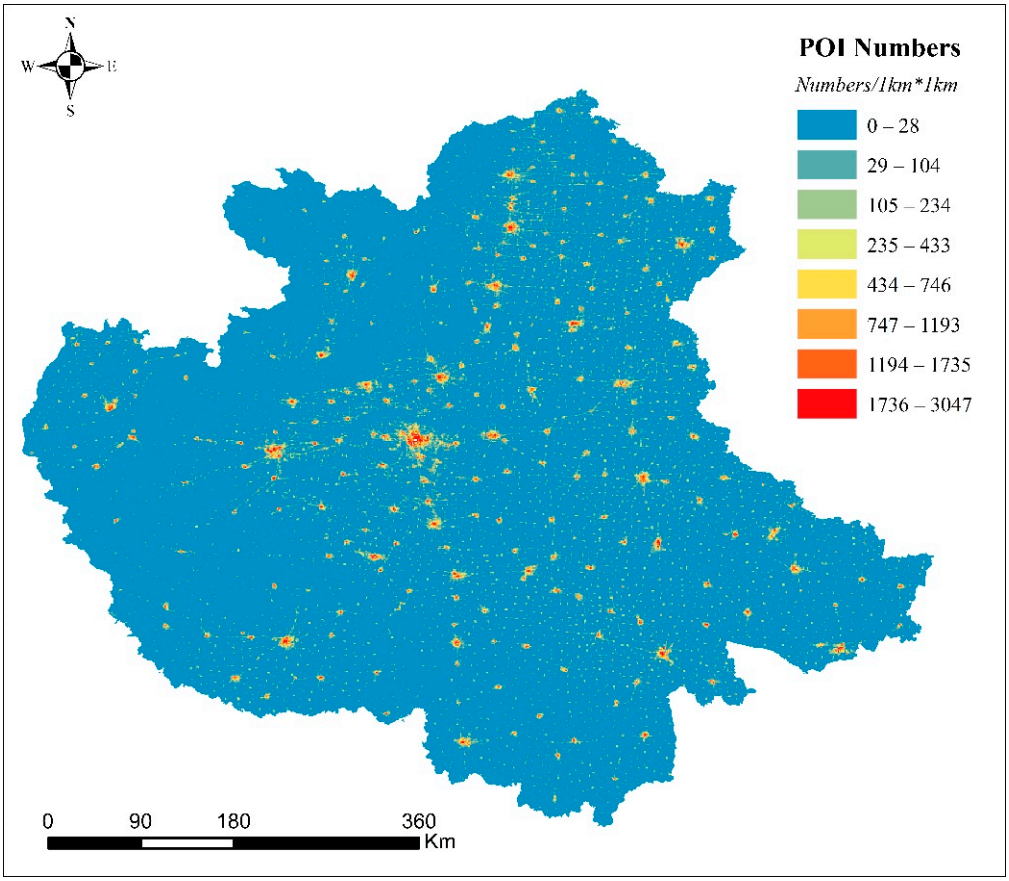

Figure 3. The Quantity and Spatial Distribution of POI Data in CPUA.

2.3. Methods

2.3.1. Wavelet Transform (WT)

As an image transformation analysis method, WT inherits and develops the localization idea of short-time Fourier transform (STFT), and overcomes the shortcomings of the STFT (the size of STFT window could not change with frequency) by providing a "time-frequency" dynamic window that changes with frequency to fuse different images [51]. In other words, WT is a representation between the function time domain (spatial domain) and frequency. With its "microscope" focusing function, it is possible to achieve the unification of the time domain and frequency domain. Wavelet analysis has good localization properties in both the time domain and frequency domain. Wavelet analysis highlights some features of the image through the "time-frequency" window and a local "focusing" analysis of time (space) frequency, which can decompose a signal into an independent part of the signal to space and time without losing the information contained in the original signal, so that the image can achieve the best observation effect after fusion. The basic formula of the wavelet transform is described as follows:

$$WT(\alpha, \tau) = f(t)\varphi(t) = \frac{1}{\sqrt{\alpha}} f(t) \int_{-\infty}^{+\infty} \varphi\left(\frac{t-b}{\alpha}\right) dt \quad (1)$$

where, a signal vector $f(t)$ can be transformed into a wavelet through the basic wavelet function ($\varphi(t)$) under the changes in different scales α, translation τ and parameters b. In this study, the wavelet transform and decomposition of NTL data and POI data are realized by OpenCV (OpenCV is a cross-platform computer vision and machine learning software library based on Apache2.0 license).

2.3.2. Object-Oriented Image Segmentation

At present, object-oriented image segmentation is the most accurate method to extract image information. Image segmentation can not only group the pixel layers of image information to form segmentation object layer, but also can further subdivide the existing segmentation object to get a new segmentation object layer.

By merging adjacent elements or segmented objects, multi-resolution segmentation uses the region merging method to complete image segmentation on the premise of ensuring the minimum average heterogeneity among objects and maximum intersegment homogeneity within an object [52]. Therefore, it is a bottom-up method.

$$\overline{C}_k = \frac{1}{n}\sum_{i=1}^{n} C_i \tag{2}$$

$$\overline{C}_k = \frac{1}{m}\sum_{k=1}^{m} \overline{C}_K \tag{3}$$

$$S^2 = \frac{1}{m}\sum_{k=1}^{m} (\overline{C}_k - \overline{C})^2 \tag{4}$$

where n is the number of pixels in the segmented image, $\overline{C}_i$ is the DN (Digital Numbers) value of the i pixel in the k segment, m is the total number of pixels in the segmented image, and S^2 is the weighted mean variance in the DN value of the segmented image.

As a segmentation optimization method, spectral difference segmentation (SDS) could decide to merge objects or not by judging and analyzing whether the brightness differences between adjacent segmented objects meet the given threshold value on the basis of multi-resolution segmentation and ESP [53]. After merging, the fragmentation of segmented images could be greatly improved, thus contributes to a higher generalization of image segmentation. The formula of SDS after normalizing weights of bands is as follows:

$$S_{diff} = \frac{\sum_k w_k}{w}\left(\frac{1}{n}\sum_n b_n - \frac{1}{m}\sum_m b_m\right) \tag{5}$$

where, S_{diff} is the spectral differences difference value between adjacent objects, k is the number of bands, w_k is the weight of kth band, w is the sum of all bands weight, n and m stand for the sum of pixels within adjacent objects, respectively, b_n and b_m are the gray value of nth pixel and mth pixel within adjacent objects. Among which, S_{diff} is the only parameter of the SDS algorithm, the bigger the value is, the easier the merge of adjacent objects will be.

Finally, eCongnition is used in this study to make the operation of multi-resolution segmentation and spectral difference segmentation simpler and more convenient.

2.3.3. Accuracy Verification

In order to verify the accuracy of the result identified by the fused NTL&POI data on the scope of CPUA, this study confirmed the accuracy of the spatial space of urban agglomerations divided by different data through the confusion matrix, whose formula is as follows:

$$k = \frac{p_o - p_e}{1 - p_e} \tag{6}$$

$$p_e = \frac{a_1 \times b_1 + a_2 \times b_2 + \ldots\ldots a_i \times b_i}{n \times n} \tag{7}$$

where, p_o is the overall accuracy, a is the real sample number for each category, b is the predicted sample number for each category, and n is the total sample number.

The technical route for identifying the spatial scope of urban agglomerations in this study is shown in Figure 4.

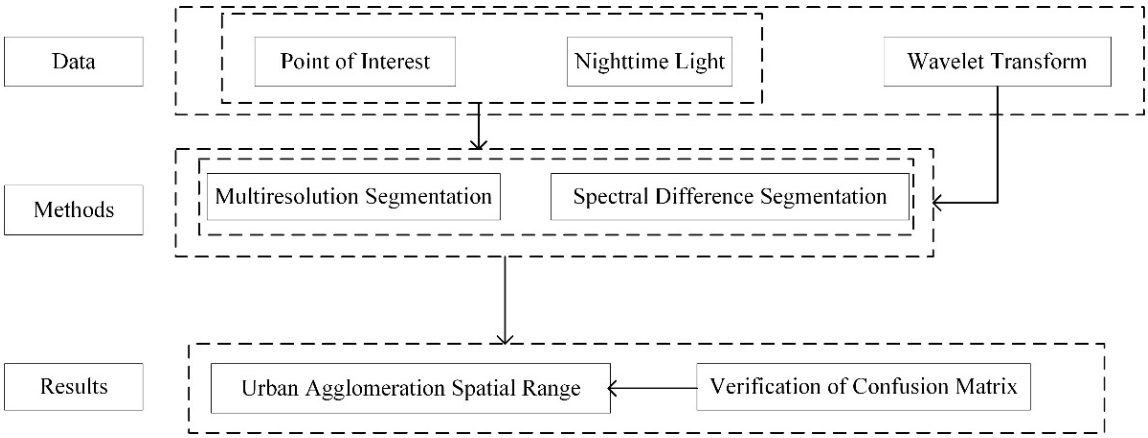

Figure 4. Technical Route of the Study.

3. Results

3.1. Spatial Area of CPUA Identified by POI Data

The quantity and spatial distribution of POI data in CPUA are shown in Figure 3. As can be seen from Figure 3, firstly, although there are plenty of agglomeration areas of POI, the spatial distribution of POI data in CPUA is relatively scattered. Secondly, high POI values are mainly concentrated in the central region with Zhengzhou as the center, covering Zhengzhou, Luoyang, Kaifeng and other places, and a high value zone of POI with Zhengzhou as the center and running through the north and South has also been formed within CPUA; Thirdly, the second highest POI value are mainly distributed in the north of the inter-regional coordinated development demonstration area dominated by Handan and Anyang. While the POI values of the southern high-efficiency ecological demonstration area, the Western transformation and innovation development demonstration area and the eastern industrial transfer demonstration area are relatively low. Therefore, it can be concluded from the spatial distribution of the high and low values of POI data that the spatial system of multi-center development of the urban agglomeration dominated by Zhengzhou, Luoyang and Kaifeng has initially formed within CPUA, while other cities have shown a trend of group dispersion and slow development, and the overall development level of CPUA could only be graded as middle.

In this study, the object-oriented image segmentation method is firstly used to identify the spatial area obtained by combining with the distribution image of POI data within CPUA on the basis of eCongnition, the identified CPUA spatial area obtained by using multi-resolution segmentation and SDS is shown in Figure 5. As can be seen from Figure 5, the urban agglomeration in CPUA identified by POI data covers an area of 7400 km^2, accounting for 2.58% of the administrative area, indicating a low level of urban agglomeration development. Through further analysis of the spatial area of the urban built-up area identified by the POI data, it can be found that the core area of CPUA is mainly concentrated in Zhengzhou, Luoyang and Kaifeng, which are also areas with a higher level of urbanization within CPUA. As for the other cities with general development levels, such as Shangqiu, Zhoukou, Bozhou, Heze, Puyang, Sanmenxia, Yuncheng, there are only a small part of the urban center have been identified by POI data. Additionally, although the number of identified urban cluster plaques is 412, except for Zhengzhou, Luoyang, other identified urban cluster plaques are generally smaller. In general, the urban agglomeration identified by POI data has a small area and a large number of urban cluster plaques. In addition, Zhengzhou has the highest level of development in CPUA, while other cities have a general level of development and weak interconnection with each other, reflecting the overall low level of development of CPUA.

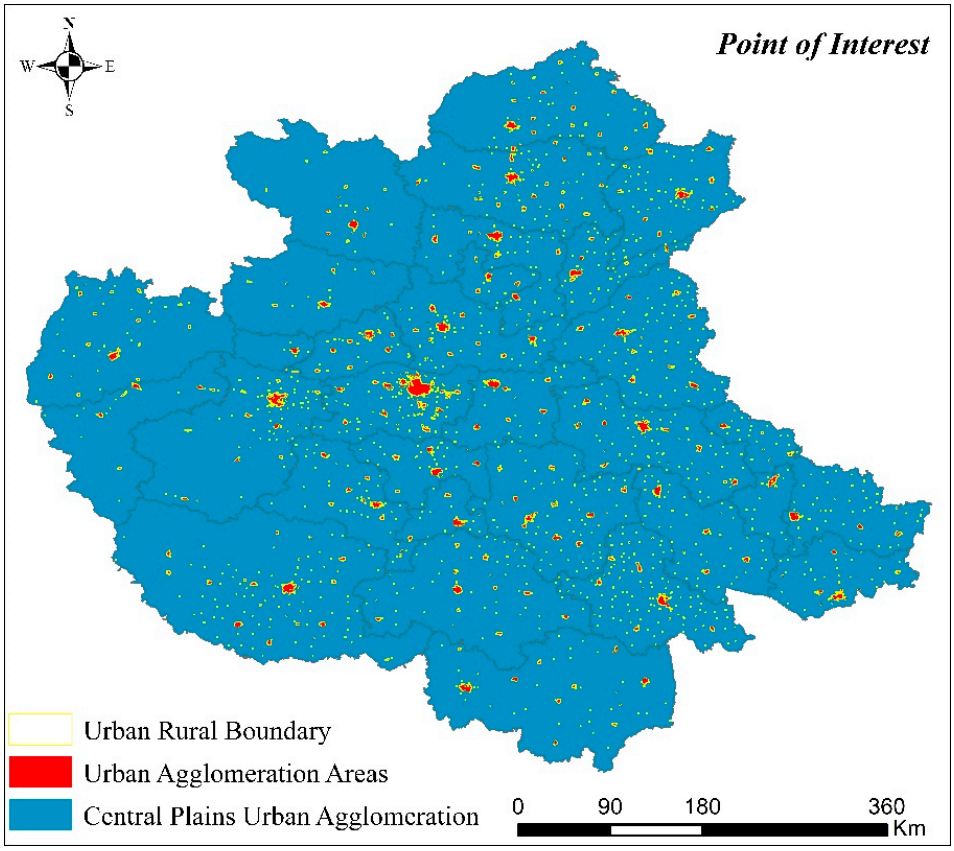

Figure 5. Spatial Area of CPUA Identified by POI Data.

3.2. Spatial Area of CPUA Identified by NPP/VIIRS Data

The pre-processing results of NPP/VIIRS NTL data are shown in Figure 2; it can be seen from Figure 2 that, firstly, although the distribution of nighttime light in CPUA is relatively concentrated, the local fragmentation phenomenon is obvious, and the overall coordination ability of CPUA reflected by NTL data is weak. Secondly, the high NTL values are mainly concentrated in 2 regions including the central region with Zhengzhou as the center, covering Zhengzhou, Luoyang, Kaifeng and other places, as well as the northern cross-regional coordinated development demonstration zone dominated by Handan and Anyang. While the NTL values of the western transformation and innovation development demonstration zone dominated by Sanmenxia and Yuncheng, the southern high-efficiency ecological demonstration zone dominated by Nanyang and Xinyang, and the eastern industrial transfer demonstration zone dominated by Fuyang and Suzhou are relatively low. Therefore, from the spatial distribution of NTL high and low values and the brightness of NTL, as can be seen the overall development level of CPUA is general and there are significant spatial differences in the development levels of different cities within the urban agglomeration; this spatial difference is manifested as the core development area centered on Zhengzhou, and multiple cities developing freely, with lower awareness of regional integration and spatial coordination.

In this study, the object-oriented image segmentation method is also used to identify the spatial area obtained by combining with the distribution image of NTL data within CPUA on the basis of eCongnition, the identified CPUA spatial area obtained by using multi-resolution segmentation and SDS is shown in Figure 6. As can be seen from Figure 6, the urban agglomeration in CPUA identified by NTL data covers an area of 8300 km^2, accounting for 2.89% of the administrative area. Although the area identified by NTL data is larger than that identified by POI data, it is not significant. Through further analysis of the spatial area of the urban built-up area identified by NTL data, it can be found that the core area of CPUA is mainly concentrated in Zhengzhou and Luoyang, which are

also areas with a higher level of urbanization within CPUA reflected by NTL data. As for the other cities with general development levels, such as Hebi, Fuyang, Anyang, there are only a small area have been identified by POI data. By comparatively analyzing the spatial distribution with the spatial area of CPUA identified by NTL data, it can be found that the spatial area of identification is basically the area with high NTL values, which makes the regions with higher development level within CPUA form an obvious contrast with the cities with average development level. Additionally, the number of urban cluster patches identified by NTL data is 361, which is lower than that identified by POI data. Comparing the spatial influence range of the CPUA identified by NTL data compared with that identified by POI data, it can be found that although the identified area of the spatial influence range and the number of urban cluster plaques identified by the two kinds of data are roughly equal, and both reflect a same fact, that is, the overall development level of CPUA is general, the POI data identifies more urban clusters, which tend to be far from the urban core, while the spatial area identified by NTL data is more concentrated on the edge of the urban core. Therefore, it can be concluded that the identification results of these two data have obvious differences.

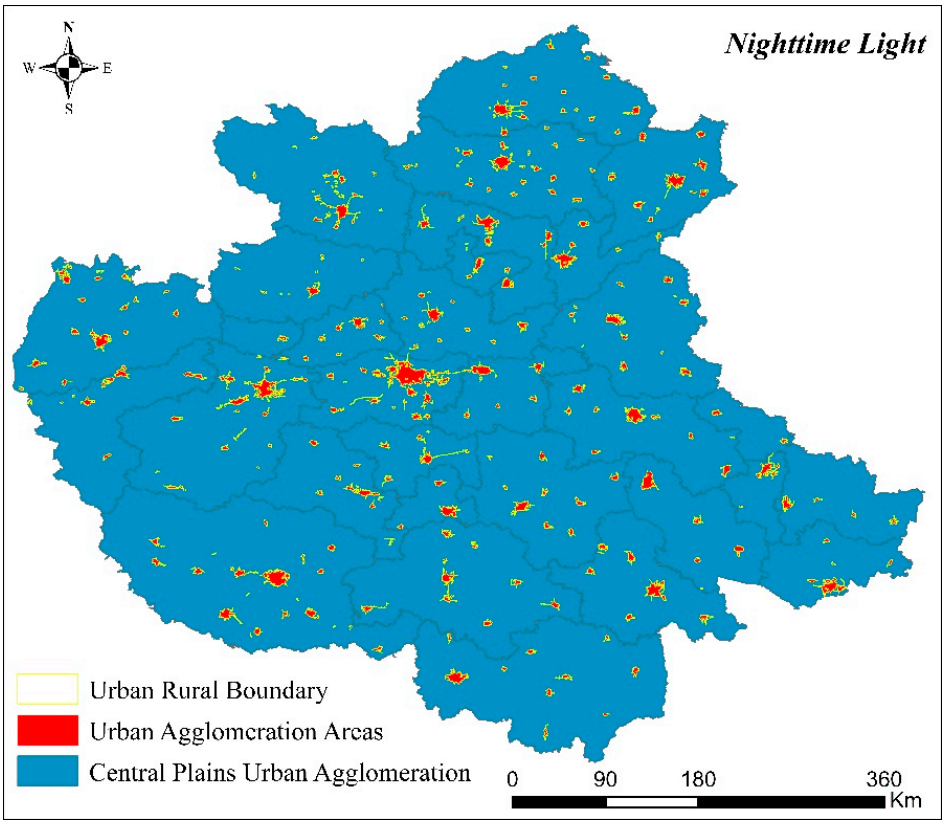

Figure 6. Spatial Area of CPUA Identified by NTL Data.

3.3. Spatial Area of CPUA Identified by Data Fusion

POI data is expressed as a point vector data set within GIS, which can be used to express the density distribution of infrastructure within a city through spatial analysis and the calculation of data volume and aggregation degree. In other words, the more the POI data, the more concentrated the POI data in a region, the more obvious the urban function of the region. While on the other hand, NTL data could reflect the differences in the activities of the urban space by capturing the difference in light brightness within the city. Therefore, there is a certain spatial correlation between the two kinds of data in the urban space, which is also shown and proved by similar studies [54]. Additionally, in this study, the spatial distribution of POI and NTL data in Figures 2 and 3 also shows the spatial correlation between them. Therefore, it is possible to identify the area of spatial influence

of urban agglomerations by fusing POI and NTL data since POI data mainly highlights urban functions, while NTL data reflects the spatial differences of urban development.

Wavelet transform is firstly used to fuse POI data and NTL data at pixel scale, and the obtained data fusion result NTL&POI (NP) is shown in Figure 7. As can be seen from Figure 7, firstly, the high value of NP is mainly distributed in the central and western regions with Zhengzhou and Luoyang as the development core, while the low value is mainly distributed in the east and west sides and southern parts of CPUA. Secondly, although the spatial distribution of NP high and low values is similar with that of POI data and NTL data on the whole, the high-value agglomeration of NP is more obvious and the urban spatial development level reflected by NP is also higher. Then multi-resolution segmentation and SDS are also used here to identify CPUA spatial area, the obtained result by using NP data is shown in Figure 8; it can be seen from Figure 6 that the urban agglomeration in CPUA identified by NP data covers an area of 11,400 km^2, accounting for 3.97% of the administrative area. As can be seen the area identified by NP data is obviously larger than that identified by both POI data and NTL data. Through further analysis of the spatial area of the urban built-up area identified by NP data, it can be found that, firstly, although the spatial area of CPUA identified after data fusion are similar with that identified by NTL data and POI data, the coverage area is wider, mainly concentrated in the northern cross-regional coordinated development demonstration areas dominated by Zhengzhou, Luoyang, Kaifeng, Handan and Anyang. Secondly, although the number of cluster patches identified by NP data after data fusion is almost the same as that identified by POI data and NTL data—388 patches, compared with the other two data, the development level of urban agglomerations reflected by NP data is slightly improved, and the identified spatial area of NP data is more concentrated near urban centers. Additionally, after data fusion, there are obvious synergies in the development of different urban clusters. Therefore, in general, the spatial area of urban agglomeration identified after data fusion is better.

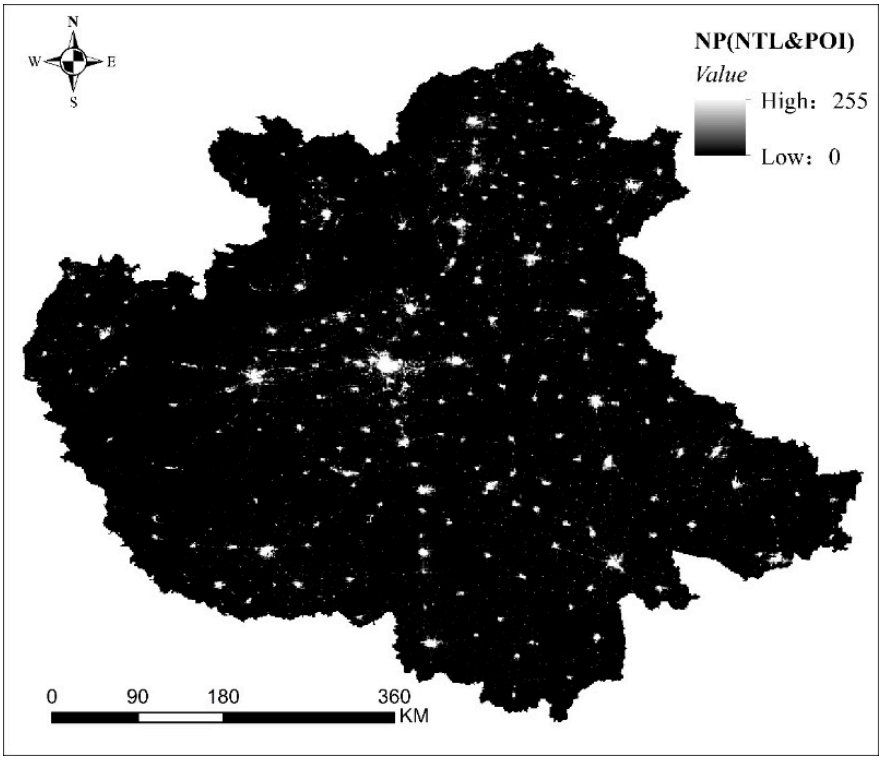

Figure 7. Fusion Results of POI Data and NTL Data.

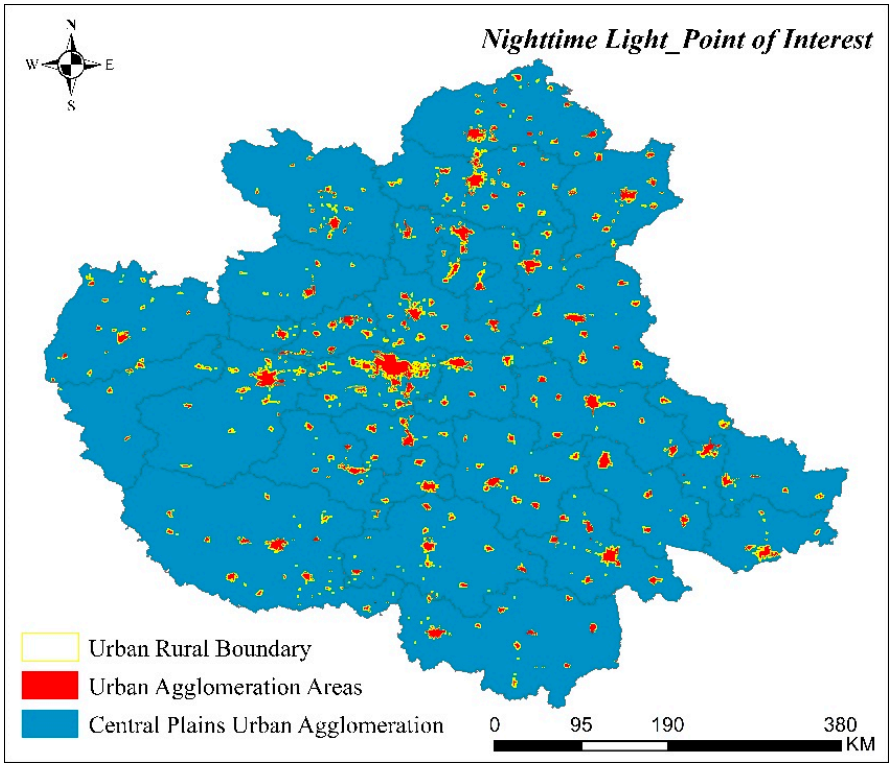

Figure 8. Spatial Area of CPUA Identified by Data Fusion.

3.4. Comparatively Verification of Spatial Area in CPUA Identified by Different Data

3.4.1. Comparison before and after Data Fusion

By analyzing Figure 9 (comparison of different data before and after fusion), it can be found that spatial area of CPUA identified by POI data, NTL data and NP data has two similarities. Firstly, the spatial structure identified by the three types of data is similar, that is, within the urban agglomeration, the values of the three types of data show a slow downward trend from high to low from different urban centers to urban edges and finally to rural areas. Secondly, the high-value areas of POI, NTL and NP are mainly concentrated in the central and western regions dominated by Zhengzhou and Luoyang, as well as high value zone with Zhengzhou as the center and running through the north and South of CPUA. These all show that POI data, NTL data and NP data can all reflect the basic spatial structure of urban agglomerations. In addition to the similarities mentioned above, there are also differences among the three.

Firstly, since the POI data reflects the urban functions of different regions in the urban agglomeration, the spatial area identified by the POI data would largely depend on the urban construction of the region; however, in the whole urban agglomeration, although there undoubtedly will be a certain degree of construction among cities in addition to the main construction of urban centers, the spatial area identified by POI data around the city would still be weakened to a certain extent. While NP data can introduce NTL data features on the basis of preserving POI data features, which strengthens the urban spatial area identified near the main urban built-up areas in the urban agglomeration, and weakens the urban development cluster between cities.

As for the differences between NP data and NTL data, since the only attribute of NTL data is the attribute of nighttime light brightness, when identifying the spatial influence range of urban agglomeration, NTL data takes the brightness value of nighttime light as the only basis to judge the influence range of a certain region, which will also cause certain errors in the identification. Additionally, due to the fact that the development level of CPUA is not high and there is a certain distance among different cities in the urban agglomeration, the NTL data is relatively isolated in space. What's more, at night, the

light is too weak to be captured among cities leads to the fact that the spatial influence range of these areas is not identified by NTL data, which makes the spatial range of urban agglomeration identified by NTL data more fragmented; however, after fusing POI data, NP data further considers the functional development of the city on the basis of light brightness, and the spatial distribution of NP high and low value is more in line with the regional differentiation of CPUA.

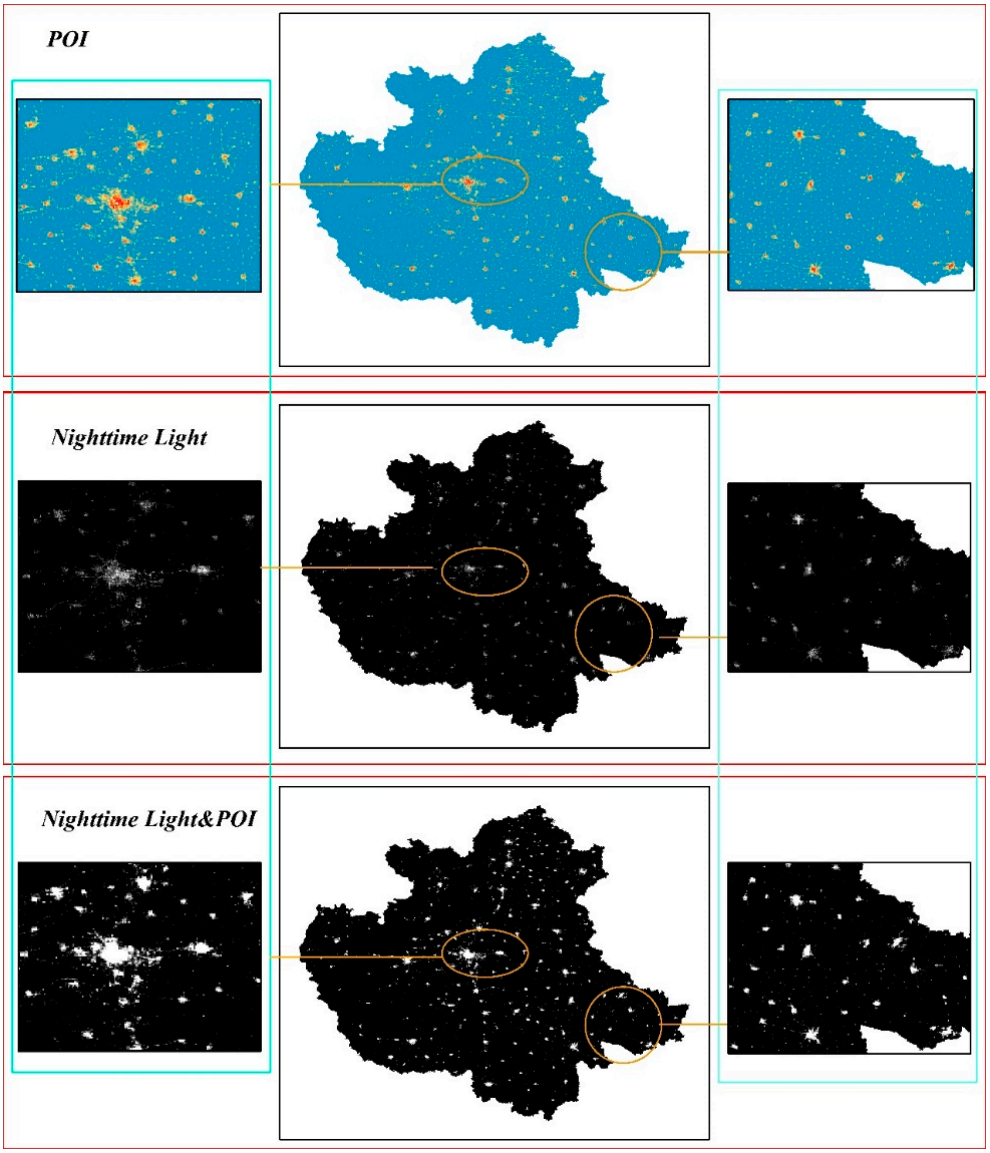

Figure 9. Comparison of Different Data Before and After Fusion.

3.4.2. Comparative Analysis of Identification Results of Spatial Area in CPUA

As shown in the spatial results of CPUA identified by different data (Figure 10), the areas of CPUA identified by POI, NTL, and NP data are 7400 km^2, 8300 km^2, and 11,400 km^2 respectively, accounting for 2.58%, 2.89%, and 3.97% of the total administrative area. From the perspective of the area of the identified spatial range, there is an obvious improvement after data fusion. From the perspective of the number of spatial clusters identified by different data, the number of clusters identified by POI, NTL, and NP data are 412, 363, and 388, respectively, among which, the spatial range identified by POI data is the most fragmented.

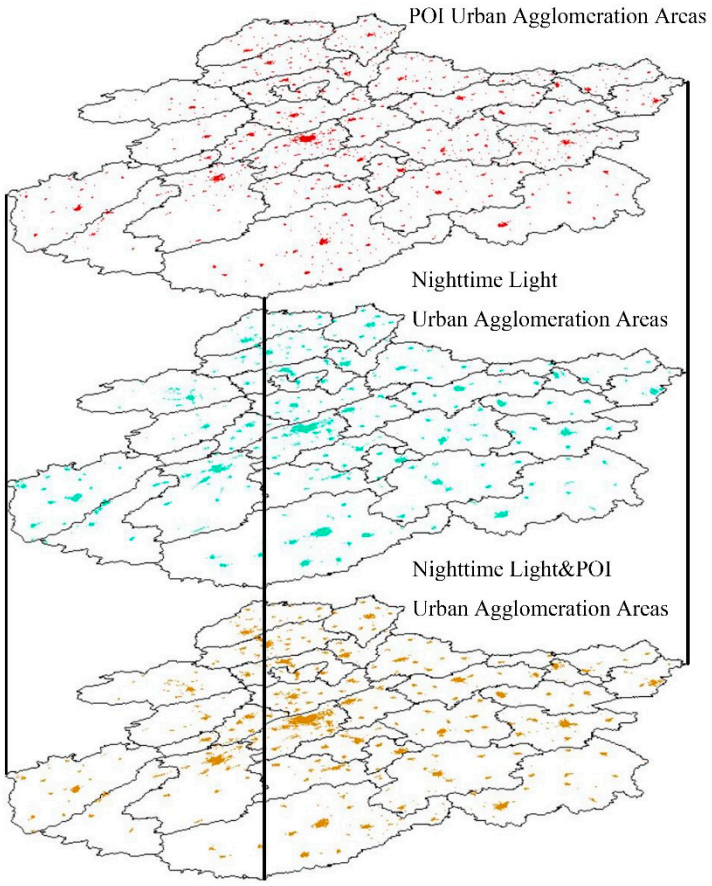

Figure 10. Comparison of Results Identified by Different Data.

By comparing the spatial area of urban agglomerations identified before and after data fusion, it can be found that POI data focuses more on identifying the functional distribution range of cities, which leads to the spatial area of urban agglomerations identified by POI data more concentrated on the functional clusters among cities. While on the other hand, NTL data pays more attention on identifying major developed areas and areas with high urbanization levels, which leads to the urban spatial area identified by NTL data more concentrated near the urban center. The NP data after data fusion has the advantages of both POI data and NTL data, which can not only highlight the highly developed urban clusters, but also can strengthen and polarize the position of urban center, making the identified spatial area more in line with the development reality of CPUA.

In general, although NTL data, POI data and the fused NTL&POI data can identify the spatial area of urban agglomerations, the spatial influence range identified by single NTL data and POI data does not take into account the functional connection among cities and the polarization effect of urban centers, which makes the spatial area identified by single data differ greatly from the actual situation. Fortunately, the fused NP data makes up for the insufficiency of NTL data and POI data, making the identification area more complete and the details more abundant.

3.4.3. Accuracy Verification

In this study, 2000 random pixel points (1000 test points and 1000 verification points) in are selected to verify the spatial area identified by different data, of which 1000 random pixel points are placed in urban areas and non-urban areas respectively. The confusion matrix obtained according to the results of random pixel point verification is shown in Table 1, where the overall accuracy and Kappa coefficient represent the accuracy of verification, which means the higher the overall accuracy and Kappa coefficient are, the higher the accuracy of identification is.

Table 1. Results of Confusion Matrix.

Data		Urban	Rural	Accuracy	Kappa
NTL	Urban	417	88	82.90%	0.6563
	Rural	83	412		
POI	Urban	401	82	81.90%	0.6441
	Rural	99	418		
NTL_POI	Urban	458	51	90.70%	0.8123
	Rural	42	449		

As shown in Table 1, the accuracy of urban agglomeration spatial areas identified by POI, NTL and NP data are 82.90%, 81.90% and 90.70% respectively, of which POI data has the lowest identification accuracy, and NP data has the highest. On the other hand, from the perspective of Kappa coefficients of POI, NTL and NP data identification results, the Kappa coefficients of POI, NTL and NP data are 0.6563, 0.6441 and 0.8123 respectively. Compared with POI data and NTL data, the Kappa coefficients of NP data had obvious advantages. In general, the fused NP data has higher accuracy in identifying the spatial area of urban agglomerations.

4. Discussion

In this study, firstly, the characteristics of POI data and NTL data in urban space were analyzed, and then the spatial area of CPUA is identified by using WT to fuse POI data and NTL data on the basis of analyzing the advantages and disadvantages of NTL data and POI data in identifying the spatial area of urban agglomerations. Finally, in combination with comparison and verification analysis, it is further confirmed that data fusion is more superior in identifying the spatial area of urban agglomeration.

Although POI data and NTL data are important basic data for urban-related studies, with the continuous in-depth study of these two data, it is found that POI data and NTL data have certain deficiencies in the application process of urban space, resulting in limited improvement of identification accuracy [54]. Therefore, researchers begin to fuse POI data and NTL data by combining with the strong spatial correlation between these two data in relevant studies [40,55]. Additionally, it has been shown by most studies that the fusion of POI data and NTL data has achieved good results by making up for each other's deficiencies thus greatly improving the study accuracy [56,57]. In this study, to obtain a more accurate spatial area of CPUA, the advantages of POI data and NTL data are fused on the premise of highlighting the internal functional development and urbanization level of urban agglomerations. The identification accuracy of this study has reached 90.70%, which has basically exceeded the accuracy of relevant studies [58]. In 2022, the built-up area of CPUA is 8500 km^2, while expecting for the area identified after data fusion to be greater than 8500 km^2, the spatial area identified by both POI data and NTL data are smaller than the actual built-up area, so it can be concluded that the spatial area of the urban agglomeration after data fusion is more inclined to the "spatial influence range of urban agglomeration".

The traditional identification of urban area simply distinguishes urban area from non-urban area (rural area), but now, as an important growth pole of regional economy, urban agglomeration is not only related to rapid urbanization, but also related to agricultural modernization, which is manifested in the fact that rural areas are also developing towards urbanization, the most prominent manifestation is the increase of rural construction land [59,60]. In this case, the simple identification of urban-rural area can no longer provide useful information for urban planners and decision-makers, so this study identifies the "used" space, which to some extent deviates from the geographical boundaries, so that urban planners and decision-makers can formulate countermeasures for urban development and management based on the status of used spaces in different areas of urban space, which are more targeted.

4.1. Study Distribution

The traditional studies on urban space and urban agglomeration space are mainly based on statistical indicators and census data under administrative divisions [61]. While with the wide application of geospatial data in recent years, the study on urban agglomeration space has made great progress [62]; however, both NTL data and POI have a certain one-sidedness, which has been ignored by most studies [57]. Therefore, based on the spatial characteristics of these two kinds of data, this study fuses POI data and NTL data to make the identification results more accurate in the identification of urban space, which provides a new method and idea for the study of urban space. Additionally, compared with other urban agglomeration studies that use NTL data and POI data to analyze urban areas, this study further verifies the applicability of the method system proposed in this study in different urban development levels through the case study of CPUA, highlighting the important value of this study. On the other hand, the space used in the city reflected by the POI data is no longer simply regarded as a supplement to the NTL data, which provides a new perspective for data fusion in the study of urban space.

4.2. Study Limitations

Although this study identifies a more accurate spatial area of CPUA after data fusion, it still has some limitations. Firstly, although the scientificity and applicability of the method proposed in this study are further proved, whether the method system proposed in this study is applicable to urban agglomerations with different development levels needs to be further verified. In addition, in this study, whether there is a significant difference between the used urban space represented by POI data and the urban space expressed by NTL data has not been analyzed in detail. Therefore, in the following study, it is necessary to carry out the analysis of different urban agglomerations in different periods, and the comparative analysis of different results to propose rapid development solutions suitable for different cities.

5. Conclusions

The accurate identification of urban agglomeration spatial range plays an important role in judging urban expansion and evaluating the development level of urban agglomeration. Based on the spatial characteristics of NTL data and POI data, this study proposes a feasible method to fuse these two data to identify the spatial area of CPUA. By carrying out the accuracy comparison and verification, it is found that the accuracy of NTL data in identifying the spatial area of urban agglomeration is 82.90%, with the kappa coefficient of 0.6563, the accuracy of POI data is 81.90%, with the kappa coefficient of 0.6441, while the accuracy after data fusion is 90.70%, with the kappa coefficient of 0.8123. Therefore, it can be concluded that the fusion of NTL data and POI data can focus on the analysis of the main impact of the urbanization level of urban agglomerations but also can supplement the analysis of various urban functions of urban agglomerations, which makes the spatial area of urban agglomerations identified after data fusion not only more accurate but also more likely to identify the "used" urban agglomeration area, which is of positive significance to the actual urban planning and management.

Author Contributions: Data curation, Shuai Zhang; Formal analysis, Shuai Zhang; Methodology, Hua Wei; Validation, Hua Wei; Visualization, Hua Wei; Writing—original draft, Shuai Zhang and Hua Wei; Writing—review and editing, Shuai Zhang. All authors have read and agreed to the published version of the manuscript.

Funding: This research was funded by [Research on the development status and construction mode of Innovation block] grant number [222400410013] And The APC was funded by [222400410013].

Institutional Review Board Statement: The study did not require ethical approval, so chose to exclude this statement.

Informed Consent Statement: The study did not involve humans, so chose to exclude this statement.

Data Availability Statement: The study did not report any data, so chose to exclude this statement.

Conflicts of Interest: The authors declare no conflict of interest.

References

1. Koopmans, S.; Ronda, R.; Steeneveld, G.J.; Holtslag, A.A.; Klein Tank, A.M. Quantifying the effect of different urban planning strategies on heat stress for current and future climates in the agglomeration of The Hague (The Netherlands). *Atmosphere* **2018**, *9*, 353. [CrossRef]
2. Rahbarianyazd, R. Cultural Agglomeration in the Urban Context: Creation and Management Approaches. *J. Urban Plan. Dev.* **2021**, *147*, 04021055. [CrossRef]
3. Blazy, R. Planning Problems and the value of the Urban and Natural Landscape Problems in the Silesian Agglomeration. In Proceedings of the IOP Conference Series: Materials Science and Engineering, Perm, Russian, 18–22 February 2019; IOP Publishing: Bristol, UK, 2019; Volume 471, p. 112012.
4. Chakraborty, S.; Maity, I.; Patel, P.P.; Dadashpoor, H.; Pramanik, S.; Follmann, A.; Novotný, J.; Roy, U. Spatio-temporal patterns of urbanization in the Kolkata Urban Agglomeration: A dynamic spatial territory-based approach. *Sustain. Cities Soc.* **2021**, *67*, 102715. [CrossRef]
5. Dong, L.; Longwu, L.; Zhenbo, W.; Liangkan, C.; Faming, Z. Exploration of coupling effects in the Economy–Society–Environment system in urban areas: Case study of the Yangtze River Delta Urban Agglomeration. *Ecol. Indic.* **2021**, *128*, 107858. [CrossRef]
6. Ahmad, M.; Khan, Z.; Anser, M.K.; Jabeen, G. Do rural-urban migration and industrial agglomeration mitigate the environmental degradation across China's regional development levels? *Sustain. Prod. Consum.* **2021**, *27*, 679–697. [CrossRef]
7. Veneri, P. City size distribution across the OECD: Does the definition of cities matter? *Comput. Environ. Urban Syst.* **2016**, *59*, 86–94. [CrossRef]
8. Kantakumar, L.N.; Kumar, S.; Schneider, K. SUSM: A scenario-based urban growth simulation model using remote sensing data. *Eur. J. Remote Sens.* **2019**, *52*, 26–41. [CrossRef]
9. Mallick, S.K.; Das, P.; Maity, B.; Rudra, S.; Pramanik, M.; Pradhan, B.; Sahana, M. Understanding future urban growth, urban resilience and sustainable development of small cities using prediction-adaptation-resilience (PAR) approach. *Sustain. Cities Soc.* **2021**, *74*, 103196. [CrossRef]
10. Nickayin, S.S.; Salvati, L.; Coluzzi, R.; Lanfredi, M.; Halbac-Cotoara-Zamfir, R.; Salvia, R.; Quaranta, G.; Alhuseen, A.; Gaburova, L. What happens in the city when long-term urban expansion and (Un) sustainable fringe development occur: The case study of Rome. *ISPRS Int. J. Geo-Inf.* **2021**, *10*, 231. [CrossRef]
11. Møller-Jensen, L.; Allotey, A.N.; Kofie, R.Y.; Yankson, P.W. A comparison of satellite-based estimates of urban agglomeration size for the Accra area. *ISPRS Int. J. Geo-Inf.* **2020**, *9*, 79. [CrossRef]
12. Pick, J.; Sarkar, A.; Rosales, J. Social media use in American counties: Geography and determinants. *ISPRS Int. J. Geo-Inf.* **2019**, *8*, 424. [CrossRef]
13. Kowe, P.; Mutanga, O.; Dube, T. Advancements in the remote sensing of landscape pattern of urban green spaces and vegetation fragmentation. *Int. J. Remote Sens.* **2021**, *42*, 3797–3832. [CrossRef]
14. Roy, B.; Kasemi, N. Monitoring urban growth dynamics using remote sensing and GIS techniques of Raiganj Urban Agglomeration, India. *Egypt. J. Remote Sens. Space Sci.* **2021**, *24*, 221–230. [CrossRef]
15. Morin, E.; Herrault, P.A.; Guinard, Y.; Grandjean, F.; Bech, N. The promising combination of a remote sensing approach and landscape connectivity modelling at a fine scale in urban planning. *Ecol. Indic.* **2022**, *139*, 108930. [CrossRef]
16. Stokes, E.C.; Seto, K.C. Characterizing urban infrastructural transitions for the Sustainable Development Goals using multi-temporal land, population, and nighttime light data. *Remote Sens. Environ.* **2019**, *234*, 111430. [CrossRef]
17. Ortakavak, Z.; Çabuk, S.N.; Cetin, M.; Senyel Kurkcuoglu, M.A.; Cabuk, A. Determination of the nighttime light imagery for urban city population using DMSP-OLS methods in Istanbul. *Environ. Monit. Assess.* **2020**, *192*, 790. [CrossRef]
18. Duque, J.C.; Lozano-Gracia, N.; Patino, J.E.; Restrepo, P.; Velasquez, W.A. Spatiotemporal dynamics of urban growth in Latin American cities: An analysis using nighttime light imagery. *Landsc. Urban Plan.* **2019**, *191*, 103640. [CrossRef]
19. Ghosh, T.; Baugh, K.E.; Elvidge, C.D.; Zhizhin, M.; Poyda, A.; Hsu, F.C. Extending the DMSP Nighttime Lights Time Series beyond 2013. *Remote Sens.* **2021**, *13*, 5004. [CrossRef]
20. Frolking, S.; Milliman, T.; Seto, K.C.; Friedl, M.A. A global fingerprint of macro-scale changes in urban structure from 1999 to 2009. *Environ. Res. Lett.* **2013**, *8*, 024004. [CrossRef]
21. Elvidge, C.D.; Zhizhin, M.; Ghosh, T.; Hsu, F.C.; Taneja, J. Annual time series of global VIIRS nighttime lights derived from monthly averages: 2012 to 2019. *Remote Sens.* **2021**, *13*, 922. [CrossRef]
22. Wang, L.; Fan, H.; Wang, Y. Improving population mapping using Luojia 1-01 nighttime light image and location-based social media data. *Sci. Total Environ.* **2020**, *730*, 139148. [CrossRef]
23. Takahashi, K.I.; Terakado, R.; Nakamura, J.; Adachi, Y.; Elvidge, C.D.; Matsuno, Y. In-use stock analysis using satellite nighttime light observation data. *Resour. Conserv. Recycl.* **2010**, *55*, 196–200. [CrossRef]
24. Mansour, S.; Alahmadi, M.; Atkinson, P.M.; Dewan, A. Forecasting of Built-Up Land Expansion in a Desert Urban Environment. *Remote Sens.* **2022**, *14*, 2037. [CrossRef]

25. Elvidge, C.D.; Zhizhin, M.; Baugh, K.; Hsu, F.C.; Ghosh, T. Extending nighttime combustion source detection limits with short wavelength VIIRS data. *Remote Sens.* **2019**, *11*, 395. [CrossRef]
26. Ghosh, T.; Elvidge, C.D.; Sutton, P.C.; Baugh, K.E.; Ziskin, D.; Tuttle, B.T. Creating a global grid of distributed fossil fuel CO_2 emissions from nighttime satellite imagery. *Energies* **2010**, *3*, 1895–1913. [CrossRef]
27. Tripathy, B.R.; Tiwari, V.; Pandey, V.; Elvidge, C.D.; Rawat, J.S.; Sharma, M.P.; Prawasi, R.; Kumar, P. Estimation of urban population dynamics using DMSP-OLS night-time lights time series sensors data. *IEEE Sens. J.* **2016**, *17*, 1013–1020. [CrossRef]
28. Miller, S.D.; Straka, I.I.I.W.; Mills, S.P.; Elvidge, C.D.; Lee, T.F.; Solbrig, J.; Walther, A.; Heidinger, A.K.; Weiss, S.C. Illuminating the capabilities of the suomi national polar-orbiting partnership (NPP) visible infrared imaging radiometer suite (VIIRS) day/night band. *Remote Sens.* **2013**, *5*, 6717–6766. [CrossRef]
29. Merlier, L.; Jacob, J.; Sagaut, P. Lattice-Boltzmann large-eddy simulation of pollutant dispersion in complex urban environment with dense gas effect: Model evaluation and flow analysis. *Build. Environ.* **2019**, *148*, 634–652. [CrossRef]
30. Mehdian, M.; Mirzahossein, H.; Abdi Kordani, A. A Data-Driven Functional Classification of Urban Roadways Based on Geometric Design, Traffic Characteristics, and Land Use Features. *J. Adv. Transp.* **2022**, *2022*, 9970464. [CrossRef]
31. Kanaroglou, P.; Mercado, R.; Maoh, H.; Paez, A.; Scott, D.M.; Newbold, B. Simulation framework for analysis of elderly mobility policies. *Transp. Res. Rec.* **2008**, *2078*, 62–71. [CrossRef]
32. Amani, M.; Ghorbanian, A.; Ahmadi, S.A.; Kakooei, M.; Moghimi, A.; Mirmazloumi, S.M.; Moghaddam, S.H.; Mahdavi, S.; Ghahremanloo, M.; Parsian, S.; et al. Google earth engine cloud computing platform for remote sensing big data applications: A comprehensive review. *IEEE J. Sel. Top. Appl. Earth Obs. Remote Sens.* **2020**, *13*, 5326–5350. [CrossRef]
33. He, X.; Zhou, C.; Zhang, J.; Yuan, X. Using wavelet transforms to fuse nighttime light data and POI big data to extract urban built-up areas. *Remote Sens.* **2020**, *12*, 3887. [CrossRef]
34. He, X.; Zhang, Z.; Yang, Z. Extraction of urban built-up area based on the fusion of night-time light data and point of interest data. *R. Soc. Open Sci.* **2021**, *8*, 210838. [CrossRef] [PubMed]
35. Guo, H.; Liu, H.; Wang, S.; Zhang, Y. An Automatic Urban Function District Division Method Based on Big Data Analysis of POI. *J. Inf. Processing Syst.* **2021**, *17*, 645–657.
36. Lou, G.; Chen, Q.; He, K.; Zhou, Y.; Shi, Z. Using nighttime light data and poi big data to detect the urban centers of hangzhou. *Remote Sens.* **2019**, *11*, 1821. [CrossRef]
37. Zhao, F.; Chu, C.; Liu, R.; Peng, Z.; Du, Q.; Xie, Z.; Sun, Z.; Zeng, H.; Xia, J. Assessing Light Pollution Using POI and Luojia1-01 Night-Time Imagery From a Quantitative Perspective at City Scale. *IEEE J. Sel. Top. Appl. Earth Obs. Remote Sens.* **2021**, *14*, 7544–7556. [CrossRef]
38. Liu, J.; Deng, Y.; Wang, Y.; Huang, H.; Du, Q.; Ren, F. Urban nighttime leisure space mapping with nighttime light images and POI data. *Remote Sens.* **2020**, *12*, 541. [CrossRef]
39. Wang, M.; Song, Y.; Wang, F.; Meng, Z. Boundary extraction of urban built-up area based on luminance value correction of NTL image. *IEEE J. Sel. Top. Appl. Earth Obs. Remote Sens.* **2021**, *14*, 7466–7477. [CrossRef]
40. Zhou, C.; He, X.; Wu, R.; Zhang, G. Using Food Delivery Data to Identify Urban-Rural Areas: A Case Study of Guangzhou, China. *Front. Earth Sci.* **2022**, *10*, 860361. [CrossRef]
41. He, X.; Cao, Y.; Zhou, C. Evaluation of polycentric spatial structure in the urban agglomeration of the pearl river delta (PRD) based on multi-source big data fusion. *Remote Sens.* **2021**, *13*, 3639. [CrossRef]
42. He, X.; Yuan, X.; Zhang, D.; Zhang, R.; Li, M.; Zhou, C. Delineation of urban agglomeration boundary based on multisource big data fusion—A case study of Guangdong–Hong Kong–Macao Greater Bay Area (GBA). *Remote Sens.* **2021**, *13*, 1801. [CrossRef]
43. Yang, X.; Ye, T.; Zhao, N.; Chen, Q.; Yue, W.; Qi, J.; Zeng, B.; Jia, P. Population mapping with multisensor remote sensing images and point-of-interest data. *Remote Sens.* **2019**, *11*, 574. [CrossRef]
44. Zhang, Z.; Zhang, Y.; He, T.; Xiao, R. Urban Vitality and its Influencing Factors: Comparative Analysis Based on Taxi Trajectory Data. *IEEE J. Sel. Top. Appl. Earth Obs. Remote Sens.* **2022**, *15*, 5102–5114. [CrossRef]
45. Hosseinpour, H.; Samadzadegan, F.; Javan, F.D. CMGFNet: A deep cross-modal gated fusion network for building extraction from very high-resolution remote sensing images. *ISPRS J. Photogramm. Remote Sens.* **2022**, *184*, 96–115. [CrossRef]
46. Allies, A.; Olioso, A.; Cappelaere, B.; Boulet, G.; Etchanchu, J.; Barral, H.; Moussa, I.B.; Chazarin, J.P.; Delogu, E.; Issoufou, H.B.; et al. A remote sensing data fusion method for continuous daily evapotranspiration mapping at kilometric scale in Sahelian areas. *J. Hydrol.* **2022**, *607*, 127504. [CrossRef]
47. Peng, J.; Ma, J.; Liu, Q.; Liu, Y.; Li, Y.; Yue, Y. Spatial-temporal change of land surface temperature across 285 cities in China: An urban-rural contrast perspective. *Sci. Total Environ.* **2018**, *635*, 487–497. [CrossRef] [PubMed]
48. Karimi, N.; Ng, K.T.W.; Richter, A. Development and application of an analytical framework for mapping probable illegal dumping sites using nighttime light imagery and various remote sensing indices. *Waste Manag.* **2022**, *143*, 195–205. [CrossRef]
49. Ivan, K.; Holobâcă, I.H.; Benedek, J.; Török, I. VIIRS nighttime light data for income estimation at local level. *Remote Sens.* **2020**, *12*, 2950. [CrossRef]
50. Lin, A.; Sun, X.; Wu, H.; Luo, W.; Wang, D.; Zhong, D.; Wang, Z.; Zhao, L.; Zhu, J. Identifying urban building function by integrating remote sensing imagery and POI data. *IEEE J. Sel. Top. Appl. Earth Obs. Remote Sens.* **2021**, *14*, 8864–8875. [CrossRef]

51. Nguyen, M.T.; Iwai, K.; Matsubara, T.; Kurokawa, T. Acceleration and higher precision by discrete wavelet transform for single image super-resolution using convolutional neural networks. In Proceedings of the 2021 Ninth International Symposium on Computing and Networking Workshops (CANDARW), Matsue, Japan, 23–26 November 2021; IEEE: Piscataway, NJ, USA, 2021; pp. 166–172.
52. Khan, S.D.; Alarabi, L.; Basalamah, S. Deep Hybrid Network for Land Cover Semantic Segmentation in High-Spatial Resolution Satellite Images. *Information* **2021**, *12*, 230. [CrossRef]
53. Niu, R.; Sun, X.; Tian, Y.; Diao, W.; Chen, K.; Fu, K. Hybrid multiple attention network for semantic segmentation in aerial images. *IEEE Trans. Geosci. Remote Sens.* **2021**, *60*, 5603018. [CrossRef]
54. Jin, C.; Zhang, Y.; Yang, X.; Zhao, N.; Ouyang, Z.; Yue, W. Mapping China's electronic power consumption using points of interest and remote sensing data. *Remote Sens.* **2021**, *13*, 1058. [CrossRef]
55. Zhou, Y.; He, X.; Zhu, Y. Identification and Evaluation of the Polycentric Urban Structure: An Empirical Analysis Based on Multi-Source Big Data Fusion. *Remote Sens.* **2022**, *14*, 2705. [CrossRef]
56. Ye, T.; Zhao, N.; Yang, X.; Ouyang, Z.; Liu, X.; Chen, Q.; Hu, K.; Yue, W.; Qi, J.; Li, Z.; et al. Improved population mapping for China using remotely sensed and points-of-interest data within a random forests model. *Sci. Total Environ.* **2019**, *658*, 936–946. [CrossRef] [PubMed]
57. Ma, T. An estimate of the pixel-level connection between visible infrared imaging radiometer suite day/night band (VIIRS DNB) nighttime lights and land features across China. *Remote Sens.* **2018**, *10*, 723. [CrossRef]
58. Shah, A.; Ali, K.; Nizami, S.M. Spatio-temporal analysis of urban sprawl in Islamabad, Pakistan during 1979–2019, using remote sensing. *GeoJournal* **2022**, *87*, 2935–2948. [CrossRef]
59. Kucharczyk, M.; Hugenholtz, C.H. Remote sensing of natural hazard-related disasters with small drones: Global trends, biases, and research opportunities. *Remote Sens. Environ.* **2021**, *264*, 112577. [CrossRef]
60. Tarolli, P.; Pijl, A.; Cucchiaro, S.; Wei, W. Slope instabilities in steep cultivation systems: Process classification and opportunities from remote sensing. *Land Degrad. Dev.* **2021**, *32*, 1368–1388. [CrossRef]
61. Nistor, C.; Vîrghileanu, M.; Cârlan, I.; Mihai, B.A.; Toma, L.; Olariu, B. Remote Sensing-Based Analysis of Urban Landscape Change in the City of Bucharest, Romania. *Remote Sens.* **2021**, *13*, 2323. [CrossRef]
62. He, X.; Zhu, Y.; Chang, P.; Zhou, C. Using Tencent User Location Data to Modify Night-Time Light Data for Delineating Urban Agglomeration Boundaries. *Front. Environ. Sci.* **2022**, *10*, 860365. [CrossRef]